

COVARIANCE FUNCTION OF ELEVATIONS

ON A CRATERED PLANETARY SURFACE

PART II

CRATER RIM AND EJECTA BLANKET CONTRIBUTION

August 6, 1968

FACILITY FORM 602

N 68-35641

(ACCESSION NUMBER)

(THRU)

31

(PAGES)

1

(CODE)

CR-97085

(NASA CR OR TMX OR AD NUMBER)

30

(CATEGORY)

Bellcomm, Inc.



COVARIANCE FUNCTION OF ELEVATIONS
ON A CRATERED PLANETARY SURFACE

PART II

CRATER RIM AND EJECTA BLANKET CONTRIBUTION

August 6, 1968

A. H. Marcus

Work performed for Office of Manned Space Flight, National
Aeronautics and Space Administration, under Contract NASW-417.

TABLE OF CONTENTS

<u>Section</u>	<u>Title</u>
	ABSTRACT
1	INTRODUCTION AND SUMMARY
2	CRATER MODEL
3	SUPERPOSITION OF ELEVATION CHANGES
4	COVARIANCE FUNCTION FOR PARABOLOIDAL CRATERS
5	THE CASE $h=\delta=1$, $k=4$
6	POWER SPECTRAL DENSITY
	REFERENCES
	TABLES

BELLCOMM. INC.

ABSTRACT

We derive the covariance function and power spectral density of elevations on a plane surface which has been excavated by paraboloidal craters with power law exterior rims and inverse power law size distribution. At moderate spatial frequencies the spectral density is an inverse power law with exponent which is a function of the parameters of the cratering process. These functions can be used to predict and/or represent the statistical roughness of surfaces similar to the lunar maria at a scale of several meters. The functions are of direct interest in vehicle mobility analyses and in interpretation of radar power returns.

BELLCOMM, INC.

COVARIANCE FUNCTION OF ELEVATIONS
ON A CRATERED PLANETARY SURFACE

PART II

CRATER RIM AND EJECTA BLANKET CONTRIBUTION

1.0 INTRODUCTION AND SUMMARY

In the first paper of this series (Marcus, 1968) hereafter called Part I, we developed the covariance function of elevations on a surface which has been excavated by craters. The only elevation changes assumed then were the negative changes due to crater bowl formation. In reality, positive relief in the form of crater rims and ejecta blankets may be important.

In this paper we study a more realistic model in which craters have paraboloidal bowls and power law exterior rims or ejecta blankets. We assume that surface elevation can be represented as a "moving average" of the Poisson stochastic point process which allocates crater centers and sizes randomly over the surface. Computational formulas are then developed for the covariance function of elevations. As in Part I, the smooth crater shape assumed implies that at small distances, the covariance function is a parabolic function of distance. At moderate distances the covariance function decreases as some power of the distance, with exponent which depends on some of the basic parameters of the cratering process. This in turn induces an inverse power law form for the power spectral density function at large and moderate spatial frequencies.

Using the most likely values of the crater parameters, some covariance functions and power spectral densities are derived numerically. These calculations provide a reasonable estimate of the statistical roughness of the non-boulder component on surfaces similar to the lunar maria, at a scale of several meters.

2.0 CRATER MODEL

As discussed in Part I, we can reasonably assume that the bowls of newborn craters are initially paraboloidal

in shape, with the initial rim-to-floor depth $H(x)$ of a crater with rim-to-rim diameter x being a power function

$$H(x) = C_0 x^\delta \quad (1)$$

For x smaller than 10 or 15 kilometers, the plausible hypothesis that crater depth is proportional to crater diameter ($\delta = 1$) is empirically verified, both for lunar craters and terrestrial explosion craters, with $C_0 = 0.25$ approximately (Baldwin, 1963). However, larger craters are shallower than predicted by the $\delta = 1$ law, requiring $\delta = 0.4$ and $C_0 = 1.3$ for $H(x)$ and x in kilometers when $x > 15$ km (Marcus, 1967). This is a consequence of both a possible change in the form of the diameter-energy scaling law for large impacts (Chabai, 1965) as well as the increasing proportion of material ejected from an impact crater which falls back into the crater as larger diameters are considered.

The shape and size of the crater rim and exterior ejecta blanket are much more poorly established than the crater depth. The initial crater rim height $R(x)$ measured from an assumed plane reference surface is assumed to also be a power law

$$R(x) = R_0 x^h \quad (2)$$

Baldwin's (1963) analysis, based on terrestrial explosion craters and some lunar craters, suggests that for $x < 10$ to 20 km, we may assume $h = 1$ and that approximately

$$R_0 = 0.055 \quad (3)$$

although the "constant" R_0 seems to increase from 0.040 at "scaled depth of burst" (DOB) = 0.00 to $R_0 = 0.090$ at DOB = 0.50. See also Carlson and Roberts (1963). The author has restudied the data, obtaining as an upper envelope for observed rims

$$R_0 = 0.085 \quad (4)$$

which in particular applies well to the assumed initial rim heights of small lunar craters. The initial rim height depends much more critically on the relative penetration of the impacting projectile and on surface mechanical properties than does the rim-to-floor depth. As the actual lunar conditions have not yet been determined, we cannot resolve the problem of the actual value of R_0 for lunar craters. The author believes $R_0 = 0.085$ is more nearly correct, but this is not yet established.

The exterior rim of the crater will be called the "ejecta blanket". In fact this consists of a layer of fragmental material ejected from the crater on top of an uplifted layer of fragmental material and cohesive substrate. We do not include as "ejecta blanket" either the fragmental "fallback" within the crater or the brecciated material beneath it. The exterior rim of a large crater is rather irregular, often described as "hummocky". An extensive analysis of the shape of the ejecta blankets of large terrestrial explosion craters has been carried out by Carlson and Roberts (1963) and Carlson and Jones (1965). They find that the height $\zeta_B(x,r)$ of the ejecta blanket from a crater of rim diameter x at a distance $r > x/2 =$ (crater radius) is a power law

$$\zeta_B(x,r) = (R_0 x^h) (2r/x)^{-k} \quad \text{if } r > x/2 \quad (5)$$

Unfortunately, a single value of k is not specified by Carlson and Jones or Roberts, but k may vary according to x or r , as is shown in Table 1. The observed values of k range from 3 to 5, but are consistent with

$$k = 4 \quad (6)$$

which is suggested by Carlson and Roberts (1963) and Carlson and Jones (1965) as the best single choice. We will use this value in calculations.

In this connection, theoretical calculations of ejecta blanket shape by Meloy and Faust (1965) may be of some interest. These are summarized in Figure 1. The power law (5) may be adequate for large craters, but small craters are

certainly scoured out by the explosive impact which formed them. The size at which this happens is of considerable interest. As Figure 1 shows, the power law shape (5) with index 2.5 is valid up to about 12 crater radii, and index 6.0 at greater distances, for diameter $x = 15.3$ meters. The approximation fails at $x = 3.3$ meters. Thus, for craters smaller than some diameter between $x = 1$ meter and $x = 10$ meters roughly, the contribution to surface elevation due to ejected debris is relatively negligible. This conclusion will be useful elsewhere. We must remember that the mathematical model used by Meloy and Faust has not been verified although it seems plausible, thus we still have some reservations about their conclusions.

A similar decrease in relative significance of the rim and ejecta blanket at diameters of less than 5 or 10 meters is observed in the extensive data on terrestrial explosion craters compiled by H. J. Moore (unpublished). The enormous variety of conditions under which the craters were formed again leaves the problem unresolved.

Combining (1), (2) and (5), we define the initial crater profile $\zeta(x,r)$ relative to the initial reference plane by

$$\begin{aligned}\zeta(x,r) &= R_0 x^h + C_0 x^\delta \left[\left(\frac{2r}{x} \right)^2 - 1 \right] && \text{for } r < x/2 \\ &= R_0 x^h \left(\frac{x}{2r} \right)^k && \text{for } r > x/2\end{aligned}\quad (7)$$

Let us compute some of the geometrical properties of the crater (7). See Figure 2 for definition of the volumes below.

$$\begin{aligned}V_I &= \text{exterior rim volume} \\ &= \frac{\pi}{8} x^3 \frac{4R_0}{(k-2)} \quad (k>2)\end{aligned}\quad (8)$$

$$\begin{aligned}V_{II} &= \text{interior rim volume} \\ &= \frac{\pi}{8} x^3 R_0^2 / C_0\end{aligned}\quad (9)$$

$$\begin{aligned}
 V_{\text{III}} &= \text{volume of true crater} \\
 &= \frac{\pi}{8} x^3 (C_o - R_o)^2 / C_o
 \end{aligned} \tag{10}$$

$$\begin{aligned}
 V_{\text{III}} + V_{\text{IV}} &= \text{volume of crater bowl} \\
 &= \frac{\pi}{8} x^3 C_o
 \end{aligned} \tag{11}$$

assuming now that

$$h = \delta = 1 \tag{12}$$

The volume coefficient in Schroter's rule* may be variously computed, for example as

$$\begin{aligned}
 &(\text{volume of rim})/(\text{volume of true crater}) \\
 &= (V_{\text{I}} + V_{\text{II}})/V_{\text{III}} \\
 &= \left[4R_o C_o / (k-2) + R_o^2 \right] / (C_o - R_o)^2
 \end{aligned} \tag{13}$$

With

$$k = 4$$

we obtain

$$\begin{aligned}
 (V_{\text{I}} + V_{\text{II}})/V_{\text{III}} &= (2R_o C_o + R_o^2) / (C_o - R_o)^2 \\
 &= 1.75 \quad \text{if } C_o = 0.25, \quad R_o = 0.085 \\
 &= 0.6865 \quad \text{if } C_o = 0.25, \quad R_o = 0.05 \\
 &= 1.00 \quad \text{if } R_o = C_o/4
 \end{aligned} \tag{14}$$

* Schroeter's rule states that $V_{\text{I}} + V_{\text{II}} = V_{\text{III}}$

We do not believe Schroter's rule is absolutely correct, as it ignores the compression of the crater bowl, uplifting of the original surface beneath the rim, and lower bulk density of breccia and fallback within the crater and of ejecta outside the crater. For further discussion of this point see Baldwin (1963), Carlson and Roberts (1963), Abrams (1966) and Pike (1967).

The probable values of R_o give reasonable results for the volume ratio. Using (7), the normal slope of the outer rim at the rim crest is

$$\tan\theta_o = -\lim_{r \rightarrow x/2} \frac{d}{dr} \zeta(x,r) = 2k R_o \cdot x^{h-1} \quad (15)$$

and the normal slope of the inner rim at the rim crest is

$$\tan\theta_i = \lim_{r \rightarrow x/2} \frac{d}{dr} \zeta(x,r) = 4C_o \cdot x^{\delta-1} \quad (16)$$

Assuming the standard parameters, we find

$$\theta_o = 34.2^\circ, \quad \theta_i = 45^\circ \quad (h=\delta=1, \quad k=4, \quad C_o=0.25, \quad R_o=0.085)$$

which are reasonable. With $R_o = 0.055$ we have $\theta_o = 23.75^\circ$.

We finally note that for $h=\delta=1$,
(diameter of true crater bowl)/(rim diameter)

$$\begin{aligned} &= \left(1 - R_o/C_o\right)^{1/2} \\ &= 0.812 \quad \text{for } C_o = 0.25, \quad R_o = 0.085 \quad (17) \\ &= 0.883 \quad \text{for } C_o = 0.25, \quad R_o = 0.055 \end{aligned}$$

compared with an observed value for fresh craters of 0.83 (Baldwin, 1963; Carlson and Roberts, 1963). Our model is reasonable in this way too.

3.0 SUPERPOSITION OF ELEVATION CHANGES

We assume that the elevation $Z(\underline{R})$ at a point \underline{R} can be represented as the sum of all the random cratering events which affect \underline{R} , either bowl or blanket formation. If we denote by $dN(x, \underline{R} + \underline{r})$ the random number of craters of diameter x to $x+dx$ formed in the small region of area $d(\underline{R} + \underline{r})$ centered on the point $\underline{R} + \underline{r}$, then our assumption can be expressed

$$Z(\underline{R}) = \int \zeta(x, r) dN(x, \underline{R} + \underline{r}) \quad (18)$$

where $r = (\text{length of } \underline{r})$. If the effects of secondary crater formation are negligible, we can assume that the primary crater process $dN(x, \underline{R} + \underline{r})$ is a Poisson point process with mean value $\xi(x)dx d(\underline{R} + \underline{r})$. $\xi(x)$ is the expected number of craters of diameter x formed per unit area per unit diameter interval, i.e., the expected number density.

We have already mentioned two difficulties with the superposition principle (18) applied to crater bowls. In the first place, we assume that the elevation change at \underline{R} due to the formation of a crater at $\underline{R} + \underline{r}$ does not depend on the elevation difference between \underline{R} and $\underline{R} + \underline{r}$ at the time the crater was formed. This is not exactly true, but is not likely to be seriously in error if surface elevations are significantly correlated at distances which are an appreciable fraction of the diameter of the largest crater affecting surface roughness; the preliminary study of Part I suggests that the significant correlation holds for a wide range of possible parameter values. A second difficulty is that the formation of a large crater will effectively erase or eliminate elevation changes at nearby points; we minimize this difficulty by choosing a distribution model in which large craters are relatively rare.

It is more reasonable to assume that ejecta blankets add linearly, since the fragmental material will simply pile up on previously existing elevations. An exception to this will occur if local slopes exceed the angle of repose of the fragmental material, whence the material will simply slide down the slope. But the model (15), (16) suggests that this will happen only on the inner wall of a crater and possibly on the outer wall near the rim crest.

In our previous paper we made an approximate correction for the effects of crater overlap. We noted then that the

formation of a large crater at a point tends to erase the contribution of the very small craters formed there. Therefore, in crater bowl-crater bowl interactions, we will use (for $x_0 < x < x_m$)

$$\xi_C(x) = \text{smaller of } \frac{2\gamma(\gamma-1)(\gamma-2)}{\pi x^3}, \frac{\gamma x_0^\gamma F}{x^{\gamma-1} [1 - (x_0/x_m)^\gamma]} \quad (19)$$

where F is the cumulative mean number of craters larger than x_0 and smaller than x_m formed per unit area, up to the present time. On the other hand, the blanket-plus-rim contribution is, on the average, not similarly "erased" by crater formation. Neither are craters likely to be lost by filling with debris ejected from other impact craters in times shorter than their lifetime with respect to loss by obliteration (overlap) by larger craters (D. Gault, personal communication). Thus, in crater-blanket and blanket-blanket interactions, we use for any F, x

$$\xi(x) = \frac{\gamma x_0^\gamma F}{x^{\gamma+1} [1 - (x_0/x_m)^\gamma]} \quad (20)$$

In applications we will consider only mare type surfaces, for which $\xi_C(x) = \xi(x)$. This approximation will be studied in more detail at some future date. In the notation of Part I, $s = \gamma$, with $2.6 < \gamma < 3.4$.

4.0 COVARIANCE FUNCTION FOR PARABOLOIDAL CRATERS

As in Part I, the representation of $Z(\underline{R})$ by a moving average of the Poisson point process $dN(x, \underline{R} + \underline{r})$

$$Z(\underline{R}) = \int \zeta(x, \underline{r}) dN(x, \underline{R} + \underline{r}) \quad (18)$$

leads to an isotropic covariance $c(\underline{r})$ between $Z(\underline{R})$ and $Z(\underline{R} + \underline{r})$, (Matern, 1960)

$$c(\underline{r}) = \int \xi(x) dx \iint \zeta(x, (u+v)/2) \zeta(x, (u-v)/2) v_2(u, v; r) du dv \quad (21)$$

where

$$v_2(u,v;r) = \frac{1}{2} \frac{u^2 - v^2}{\sqrt{u^2 - r^2} \sqrt{r^2 - v^2}} \quad \begin{array}{l} \text{for } u > r \\ \text{and } -r < v < r \end{array} \quad (22)$$

$$v_2(u,v;r) = 0 \quad \text{otherwise}$$

Using the crater profile $\zeta(x,r)$ defined by (7) we obtain

$$c(r) = \frac{C_0^2}{T_0^2} c_I(r) + \frac{1}{2} \int \xi(x) dx \{k_1(r,x) + k_2(r,x) + k_3(r,x)\} \quad (23)$$

where $c_I(r)$ is the crater bowl contribution to the covariance function, precisely Equation (47) of Part I. The other functions are:

$$k_1(r,x) = \int_r^x \frac{du}{\sqrt{u^2 - r^2}} L_1(u;x-u;r,x) \quad \text{if } r < x < 2r$$

$$k_1(r,x) = \int_r^{x-r} \frac{du}{\sqrt{u^2 - r^2}} L_1(u;r;r,x) \quad (24)$$

$$+ \int_{x-r}^x \frac{du}{\sqrt{u^2 - r^2}} L_1(u;x-u;r,x) \quad \text{if } 2r < x$$

$$k_1(r,x) = 0 \quad \text{if } 0 \leq x < r$$

$$k_2(r,x) = \int_r^{x+r} \frac{du}{\sqrt{u^2 - r^2}} L_2(u;u-x;r,x) \quad \text{if } 0 < x < r$$

$$k_2(r, x) = \int_r^x \frac{du}{\sqrt{u^2 - r^2}} L_2(u; x-u; r, x) \quad (25)$$

$$+ \int_x^{x+r} \frac{du}{\sqrt{u^2 - r^2}} L_2(u; u-x; r, x) \quad \text{if } r < x < 2r$$

$$k_2(r, x) = \int_{x-r}^x \frac{du}{\sqrt{u^2 - r^2}} L_2(u; x-u; r, x)$$

$$+ \int_x^{x+r} \frac{du}{\sqrt{u^2 - r^2}} L_2(u; u-x; r, x) \quad \text{if } 2r < x$$

$$k_3(r, x) = \int_r^{x+r} \frac{du}{\sqrt{u^2 - r^2}} L_3(u; u-x; r, x)$$

$$+ \int_{x+r}^{\infty} \frac{du}{\sqrt{u^2 - r^2}} L_3(u; r; r, x) \quad \text{if } 0 < x < r$$

$$k_3(r, x) = \int_x^{x+r} \frac{du}{\sqrt{u^2 - r^2}} L_3(u; u-x; r, x) \quad (26)$$

$$+ \int_{x+r}^{\infty} \frac{du}{\sqrt{u^2 - r^2}} L_3(u; r; r, x) \quad \text{if } x > r$$

The integrals L_1 , L_2 , L_3 are defined by:

$$L_1(u; a; r, x) = \int_{-a}^a \frac{u^2 - v^2}{\sqrt{r^2 - v^2}} \left\{ \left(R_0^2 x^{2h} - 2R_0 C_0 x^{h+\delta} \right) \right. \\ \left. + 2R_0 C_0 x^{h+\delta-2} (u^2 + v^2) \right\} dv \quad (27)$$

$$L_2(u;a;r,x) = \int_{-r}^{-a} \frac{u^2-v^2}{(u-v)^k \sqrt{r^2-v^2}} \left\{ 2R_o^2 x^{2h+k} \right. \\ \left. - 2R_o C_o x^{h+\delta+k} \left[1 - \frac{(u+v)^2}{x^2} \right] \right\} dv \quad (28)$$

$$L_3(u;a;r,x) = \int_{-a}^a \frac{R_o^2 x^{2h+2k}}{u^2-v^2} \frac{1}{k-1 \sqrt{r^2-v^2}} dv \quad (29)$$

We easily find

$$\frac{1}{2} L_1(u;a;r,x) = \arcsin\left(\frac{a}{r}\right) \left\{ (u^2-r^2)^2 2R_o C_o x^{h+\delta-2} \right. \\ + (u^2-r^2) \left[R_o^2 x^{2h} - 2R_o C_o x^{h+\delta} + 4r^2 R_o C_o \right] \\ + \frac{r^2}{2} \left[R_o^2 x^{2h} - 2R_o C_o x^{h+\delta} + \frac{5}{2} R_o C_o x^{h+\delta-2} r^2 \right] \left. \right\} \\ + \frac{a}{2} \sqrt{r^2-a^2} \left\{ R_o C_o a^2 + (R_o^2 x^{2h} - 2R_o C_o x^{h+\delta}) \right. \\ \left. + \frac{3}{2} R_o C_o x^{h+\delta-2} r^2 \right\} \quad (30)$$

The integrals L_2 and L_3 can be evaluated explicitly only for integer values of k . From Section 2 we see that k lies between 3 and 4, thus we use explicitly $k=3$ and $k=4$, obtaining:

$$(k=3) \frac{1}{2} L_2(u;a;r,x) = 2u \frac{\sqrt{r^2-a^2}}{u+a} \left\{ \frac{Q_1(x)r}{u^2-r^2} - 4Q_2(x) \right\} \\ + 5u \arccos\left(\frac{a}{r}\right) Q_2(x) \quad (31) \\ + \arccos\left[\frac{ua+r^2}{(u+a)r}\right] \left\{ \frac{(u^2+r^2)}{(u^2-r^2)^{3/2}} Q_1(x,r) \right. \\ \left. - 4\sqrt{u^2-r^2} Q_2(x) \right\}$$

where

$$Q_1(x,r) = R_0^2 x^{2h+k} - R_0 C_0 x^{h+\delta+k-2} (u^2+4r^2) \quad (32)$$

$$Q_2(x) = R_0 C_0 x^{h+\delta+k-2}$$

$$\begin{aligned} (k=4) \frac{1}{2} L_2(u;a;r,x) &= \frac{u\sqrt{r^2-a^2}}{(u+a)^2} \left\{ \frac{Q_1(x,r)}{u^2-r^2} - 4Q_2(x) \right\} \\ &+ \frac{\sqrt{r^2-a^2}}{u+a} \left\{ \frac{3r^2 Q_1(x,r)}{(u^2-r^2)^2} + \frac{2Q_1(x,r)-4r^2 Q_2(x)}{(u^2-r^2)} \right\} \\ &+ u \arccos \left[\frac{ua+r^2}{(u+a)r} \right] \left\{ \frac{3r^2 Q_1(x,r)}{(u^2-r^2)^{5/2}} + \frac{Q_1(x,r)-4r^2 Q_2(x)}{(u^2-r^2)^{3/2}} \right. \\ &\left. + \frac{10 Q_2(x)}{\sqrt{u^2-r^2}} \right\} + \arccos \left\{ \frac{a}{r} \right\} Q_2(x) \end{aligned} \quad (33)$$

Finally,

$$\begin{aligned} (k=3) \frac{1}{2} L_3(u;a;r,x) &= \frac{1}{2} R_0^2 x^{2h+2k} \left\{ \frac{(2u^2-r^2)}{u^3(u^2-r^2)^{3/2}} \arccos \left[\frac{u^2 r^2 - (2u^2-r^2)a^2}{r^2(u^2-a^2)} \right] \right. \\ &\left. - \frac{a\sqrt{r^2-a^2}}{u^2(u^2-r^2)(u^2-a^2)} \right\} \end{aligned} \quad (34)$$

$$\begin{aligned} (k=4) L_3(u;a;r,x) &= R_0^2 x^{2h+2k} \left\{ \frac{8u^4-8u^2r^2+3r^4}{8u^5(u^2-r^2)^{5/2}} \arccos \left[\frac{u^2 r^2 - (2u^2-r^2)a^2}{r^2(u^2-a^2)} \right] \right. \\ &\left. - \frac{a\sqrt{r^2-a^2} [4u^4-u^2r^2-3(2u^2-r^2)a^2]}{4u^4(u^2-r^2)^2(u^2-a^2)^2} \right\} \end{aligned} \quad (35)$$

It is clear that these functions are too complicated to permit an explicit evaluation of the k integrals, much less $c(r)$. However, $c(r)$ can be computed with suitable additional approximations and simplifications. We explore this possibility in the next section.

5.0 THE CASE $h=\delta=1, k=4$

Let us assume that vertical relief of craters is scaled in direct proportion to crater diameter, which is both intuitively appealing and experimentally verified for small craters. In terms of our model functions,

$$h=\delta=1$$

The Equation (23) for $c(r)$ now assumes a more attractive and tractable form,

$$c(r) = \frac{c_o^2}{T_o^2} C_I(r) + \frac{sCr^s}{2 \left[1 - \left(\frac{x_o}{x_m} \right)^s \right]} \int_{\max(1, x_o/r)}^{x_m/r} \frac{dy}{y^{s+1}} \left\{ k_1(r, ry) + k_2(r, ry) + k_3(r, ry) \right\} \quad (36)$$

By appropriate partial integrations,

$$k_1(r, ry) = r \int_{\max(1, y-1)}^y \left[\frac{\phi_1(w, y)}{\sqrt{1-(y-w)^2}} + \frac{\psi_1(w, y)}{\sqrt{w^2-1}} \right] dw \quad (37)$$

where

$$\phi_1(w, y) = R_o C_o w (w^2-1)^{3/2} + \frac{1}{2} w (w^2-1)^{1/2} \left[2y^2 (R_o^2 - 2R_o C_o) + 5R_o C_o \right] \quad (38)$$

$$\psi_1(w, y) = (y-w) \sqrt{1-(y-w)^2} \left[(R_o^2 - 2R_o C_o) y^2 + R_o C_o (y-w)^2 + \frac{3}{2} R_o C_o \right] \quad (39)$$

in the transformed variables

$$y = x/r \quad , \quad w = u/r \tag{40}$$

By the same transformations (40), $k_2(r,ry)$ and $k_3(r,ry)$ can also be simplified. An explicit statement requires a choice of k , however.

The most probable value,

$$k = 4 \tag{41}$$

is assumed. This yields

$$\begin{aligned} k_2(r,ry) = & 2r^4 \int_{\max(1,y-1)}^y \frac{dw}{\sqrt{w^2-1}} \left\{ \frac{w\sqrt{1-(y-w)^2}}{y^2} \phi_{21}(w,y) + \frac{\sqrt{1-(y-w)^2}}{y} \phi_{22}(w,y) \right. \\ & \left. + w \arccos \left[\frac{w(y-w)+1}{y} \right] \phi_{23}(w,y) + R_o C_o y^4 \arccos(y-w) \right\} \\ & + 2r^4 \int_y^{y+1} \frac{dw}{\sqrt{w^2-1}} \left\{ \frac{w\sqrt{1-(w-y)^2}}{(2w-y)^2} \phi_{21}(w,y) + \frac{\sqrt{1-(w-y)^2}}{2w-y} \phi_{22}(w,y) \right. \\ & \left. + w \arccos \left[\frac{w(w-y)+1}{2w-y} \right] \phi_{23}(w,y) + R_o C_o y^4 \arccos(w-y) \right\} \end{aligned} \tag{42}$$

where

$$\begin{aligned} \phi_{21}(w,y) &= \frac{(R_o^2 - R_o C_o) y^6 - 4R_o C_o y^4}{w^2 - 1} - 4R_o C_o y^3 \\ \phi_{22}(w,y) &= \frac{3[(R_o^2 - R_o C_o) y^6 - 4R_o C_o y^4]}{(w^2 - 1)^2} + \frac{2[(R_o^2 - R_o C_o) y^6 - 6R_o C_o y^4]}{w^2 - 1} \\ \phi_{23}(w,y) &= \frac{(R_o^2 - R_o C_o) y^6 - 8R_o C_o y^4}{(w^2 - 1)^{3/2}} + \frac{10 R_o C_o y^4}{\sqrt{w^2 - 1}} \\ &+ \frac{3(R_o^2 - R_o C_o) y^6 - 4R_o C_o y^4}{(w^2 - 1)^{5/2}} \end{aligned} \tag{43}$$

Also,

$$\begin{aligned}
 k_3(r,ry) = R_0^2 y^{10} r^4 & \left\{ \frac{\pi}{8} \int_{y+1}^{\infty} \frac{(8w^4 - 8w^2 + 3)}{w^5 (w^2 - 1)^3} dw \right. \\
 & + \int_y^{y+1} \frac{dw}{\sqrt{w^2 - 1}} \left[\frac{(8w^4 - 8w^2 + 3)}{8w^5 (w^2 - 1)^{5/2}} \arccos \left(\frac{w^2 - (2w^2 - 1)(w-y)^2}{w^2 - (w-y)^2} \right) \right. \\
 & \left. \left. - \frac{(y-w) \sqrt{1 - (y-w)^2} [4w^4 - w^2 - 3(2w^2 - 1)(w-y)^2]}{4w^4 (w^2 - 1)^2 [w^2 - (w-y)^2]^2} \right] \right\} \quad (44)
 \end{aligned}$$

Even without detailed computations, we may extract useful asymptotic information about $c(r)$ by developing it as a power series in r for small r :

$$c(r) = c(0) - (\text{const})r^{\mu-1} + o(r^{\mu-1}) \quad (45)$$

where

$$1 < \mu \leq 3$$

Omitting the usual involved calculations, we find that as $y \rightarrow \infty$ (x_0 fixed, $r \rightarrow 0$)

$$k_1(r,ry) + k_2(r,ry) + k_3(r,ry) = \frac{\pi}{6} r^4 y^4 [4R_0^2 - 3R_0 C_0] + r^4 O(y^2) \quad (46)$$

(We have verified that the coefficient of y^3 is identically zero, but did not undertake an exact calculation of the coefficient of y^2 .)

It was found in Part I that for $\delta = 1$

$$\begin{aligned} \frac{c_o^2}{T_o^2} C_I(r) &= \frac{s C C_o^2}{(4-s) \left[1 - \left(\frac{x_o}{x_m} \right)^s \right]} \frac{\pi}{12} \left(x_m^{4-s} - x_o^{4-s} \right) + 0(r^2) \quad \text{if } s \neq 4 \\ &= \frac{s C C_o^2}{1 - \left(\frac{x_o}{x_m} \right)^s} \frac{\pi}{12} \log \left(x_m/x_o \right) + 0(r^2) \quad \text{if } s=4 \end{aligned} \tag{47}$$

Therefore,

$$\begin{aligned} (r \rightarrow 0) \ c(r) &= \frac{\pi}{12} \frac{s C \left(x_m^{4-s} - x_o^{4-s} \right)}{(4-s) \left[1 - \left(x_o/x_m \right)^s \right]} \left(C_o^2 - 3R_o C_o + 4R_o^2 \right) + 0(r^2) \quad \text{if } s \neq 4 \\ (r \rightarrow 0) \ c(r) &= \frac{\pi}{12} \frac{s C \log \left(x_m/x_o \right)}{\left[1 - \left(x_o/x_m \right)^s \right]} \left(C_o^2 - 3R_o C_o + 4R_o^2 \right) + 0(r^2) \quad \text{if } s=4 \end{aligned} \tag{48}$$

We remark that for any C_o, R_o (either non-zero)

$$C_o^2 - 3R_o C_o + 4R_o^2 > 0 \tag{49}$$

thus $c(0) > 0$.

Equations (36) - (44) were computed numerically for $x_o = 1, x_m = 100, R_o = 0.085, C_o = 0.25$, and $s = 2, 3, 4$. The resulting correlation functions $c(r)/c(0)$ are shown in Figure 3. The character of these functions is much the same as those found in Part I. For values of r somewhat larger than x_o , the decline in $c(r)$ with increasing r is:

- (i) Parabolic for $s = 2$
- (ii) Linear (exponential) for $s = 3$
- (iii) "Logarithmic" for $s = 4$

Therefore, as found in Part I, Equation (45) is applicable for small and moderate values of r , with

$$\mu = 3 + 2\delta - s \quad (50)$$

for $s < 2 + 2\delta$, and

$$c(r) = c(0) - (\text{const}) \log r + o(\log r) \quad (51)$$

if $s = 2 + 2\delta$.

This model is "smoother" than that of Part I if $c(0) < C_I(0)$, i.e., if

$$T_0^2 = \left(C_0 - R_0 \right)^2 > \left(C_0^2 - 3C_0R_0 + 4R_0^2 \right)$$

or equivalently

$$R_0 < C_0/3$$

From Section 2, using $C_0 = 0.25$, we find that

- (a) if $R_0 = 0.085$, the present model is slightly rougher, and
- (b) if $R_0 = 0.055$, the present model is smoother than the model of Part I.

A measure of the reasonable numerical magnitude of these results is the root-mean-square elevation relative to the mean surface, $\sqrt{c(0)}$. This is plotted in Figure 4 as a function of x_m for the case $h=\delta=1$, $k=4$, $C_0=0.25$, $R_0=0.085$, and varying values of s and C . We have used $x_0 = 1$ meter, but as noted in Part I, even smaller values of x_0 contribute little extra to the total roughness if $s < 3.5$. The case $s = 2$, $C = 0.2$ is the worst possible continental distribution, the case $s = 2$,

$C = 0.08$ is the smoothed Surveyor crater distribution, and the other cases are typical mare distributions. For example, we would expect a typical Apollo landing site ($C = 0.2$, $2.5 \leq s \leq 3.0$, no craters larger than, say, $x_m = 250$ meters) to have an r.m.s. roughness of 1 to 3 meters, mostly due to crater bowls.

6.0 POWER SPECTRAL DENSITY

The two-dimensional power spectral density (PSD) $S(\omega)$ is, in the case of an isotropic surface, simply the Hankel transform of the covariance function $c(r)$

$$S(\omega) = \int_0^{\infty} J_0(\omega r) c(r) 2\pi r dr \quad (52)$$

where the spatial frequency ω is related to the distance r by $\omega = 2\pi/r$, and $J_0(z)$ is the zeroth order Bessel function. This function $S(\omega)$ has been computed numerically from the correlation functions $c(r)/c(0)$ shown in Figure 3, thus $S(\omega)$ as plotted in Figure 5 is "normalized".

These numerical results verify the asymptotic analysis of the preceding section. As was shown in Part I, if for sufficiently small values of r

$$c(r) \approx c(0) - (\text{const})r^{\mu-1} + o(r^{\mu-1})$$

where $1 < \mu < 3$, then

$$S(\omega) \approx (\text{const})\omega^{-(\mu+1)} \quad (53)$$

From Equation (50), with $\delta = 1$,

$$\mu + 1 = 6 - s \quad (54)$$

which is, indeed, verified for $0.1 < \omega < 1.0$.

Because of the truncation at $x_0 = 1$, we have in (50) for $r \ll x_0 = 1$ or equivalently, $\omega \gg 2\pi/x_0 = 2\pi$, that $\mu = 3$ and

that $S(\omega)$ decreases with increasing ω faster than ω^{-3} ; this is beginning to appear in the functions sketched in Figure 5, although not fully developed. Because $c(r) = 0$ for $r > x_m = 100$, we have $S(\omega)$ extremely flat for $\omega < 0.01$. If x_m is increased or x_0 decreased, we can expect that the inverse-power-law PSD with slope $\mu + 1 = 6 - s$ observed in this example for $0.1 < \omega < 1.0$ will extend, respectively, to smaller and to larger values of ω .

The one-dimensional PSD for elevations along a single linear traverse, denoted $S_1(\omega_1)$, is calculated from $S(\omega)$ by

$$S_1(\omega_1) = \int_{\omega_1}^{\infty} S(\omega) d\omega / (1 - \omega_1^2/\omega^2)^{1/2} \quad (55)$$

where ω_1 is the spatial frequency along the linear traverse. It is evident that if over any range of ω , Equation (53) holds then

$$S_1(\omega_1) \approx (\text{const}) \omega_1^{-\mu} \quad (56)$$

which is verified in Figure 6. For a range of values of ω_1 which depend on s , but are roughly between 0.08 and 0.80, we have (56) with $\mu = 5-s$, in accord with theoretical predictions.

The empirical estimation of $S_1(\omega_1)$ from lunar data is now being studied. Preliminary findings by Van Deusen (1967) show that (56) is applicable for $0.1 \leq \omega_1 \leq 1$ cycle/meter, with $\mu = 2$. The derived value $s = 3$ is in good agreement with the observed population index of crater diameters. A more detailed analysis will be published separately.

A H Marcus

REFERENCES

1. Abrams, W. J., (1966), An Investigation of Schröeter's Rule, Astron. Contrib. Boston Univ., Ser. 2, No. 42.
2. Baldwin, R. B., (1963), The Measure Of The Moon, Univ. Chicago Press, Chicago.
3. Carlson, R. H. and G. D. Jones, (1965), Distribution of Ejecta From Cratering Explosions, J. Geophys. Res., 70, 1897-1910.
4. Carlson, R. H. and W. A. Roberts, (1963), Mass Distribution and Throwout Studies, Final Report, Project Sedan, Boeing Co. Report D2-90457.
5. Chabai, A. J., (1965), On Scaling Dimensions of Craters Produced By Buried Explosives, J. Geophys. Res., 70, 5075-5098.
6. Marcus, A. H., (1967), Stochastic Model of The Formation and Survival of Lunar Craters-Part VI, Initial Depth, Distribution of Depths, and Lunar History, Icarus, 7, 56-78.
7. Marcus, A. H., (1968), Covariance Function of Elevations On A Cratered Planetary Surface-Part I, Crater Bowl Contribution, Bellcomm Technical Report, TR-68-340-3.
8. Matern, B. (1960), Spatial Variation, Publications of The Swedish Forestry Institute, 49, (No. 5), Stockholm.
9. Meloy, T. P. and L. H. Faust, (1965), Lunar Surface Roughness Comminution Study, Final Report From Allis-Chalmers Mfg. Co., Milwaukee, Wisc. to Jet Propulsion Lab., Pasadena, Calif., under Contract No. 950919, Serial No. 6224.
10. Pike, R. J., (1967), Schröeter's Rule and The Modification Of Lunar Crater Impact Morphology, J. Geophys. Res., 72, 2099-2106.
11. Van Deusen, B. D. (1967). "A Statistical Technique for the Dynamic Analysis of Vehicles Traversing Rough Yielding and Non-yielding Surfaces", Chrysler Corporation, Detroit, Michigan. NASA-CR-659.

TABLE 1

EJECTA BLANKET SHAPE

Shot	True Crater Radius (Meters)	k	Range (Meters)
Sedan	182.9	4.3 5.1 2.24 5.98 3.53 4.0	(all stations) (29)* (primary stations)(29)* 220 to 550 (55)* 550 to 840 (55)* 840 to 1710 (55)* suggested (72)*
Teapot S	44.5	3.7 0.0 4.31 3.57 4.5	suggested (72)* 53 to 65 ** 65 to 245 ** 245 to 2650 ** ***
Scooter	38.1	2.6 6.51 4.05 2.7	457 to 980 (13)* 122 to 172 ** 172 to ∞ ** ***
Suffield	21.3	3.65	30 to 73 **
Stagecoach 2	15.4	4.75 2.40 4.25	30 to 73 ** 73 to ∞ ** 30 to 60 ***
Stagecoach 3	17.9	2.35 3.28 3.74	73 to 334 (13)* 43 to ∞ ** 43 to ∞ ***
White Tribe (average, 9 shots)	5.3	2.73	15 to 167

*Carlson and Robert (1963), page number

**Carlson and Jones (1965)

***Marcus, unpublished

CAPTIONS TO FIGURES

- Figure 1 Theoretical estimate of height of ejecta blanket around a crater of diameter x formed by an impact of energy E , as a function of distance from crater center (Meloy and Faust, 1965).
- Figure 2 Possible crater shapes for various model parameter values (drawn to scale).
- Figure 3 Correlation functions.
- Figure 4 R.M.S. surface elevation as a function of maximum crater size for $x_0 = 1$ meter, $h = \delta = 1$, $k = 4$, $C_0 = 0.25$ and $R_0 = 0.085$. s is the population index and C the number of craters per square meter larger than one meter in diameter.
- Figures 5-6 Power spectral density functions corresponding to the correlation functions in Figure 3.

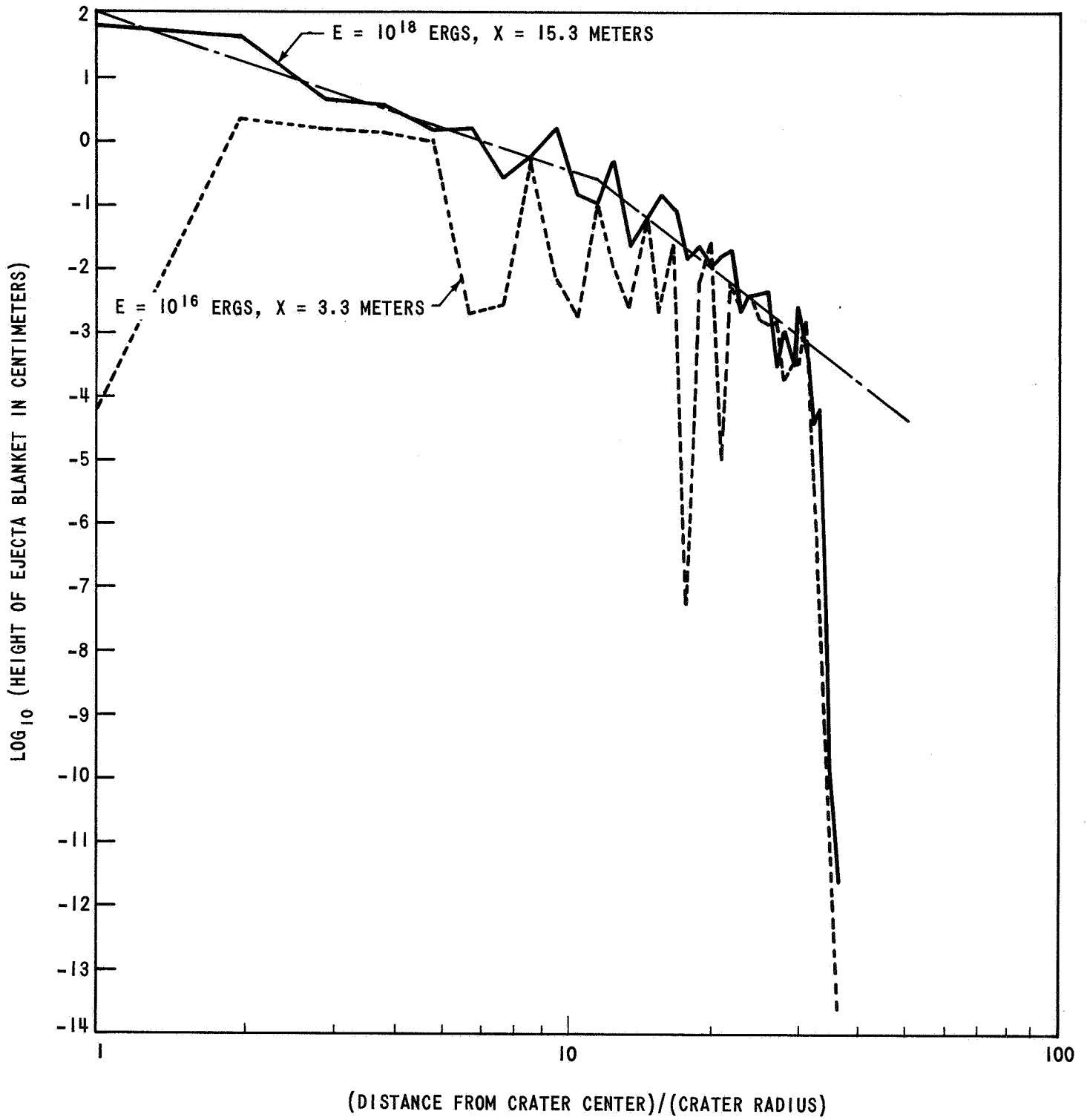


FIGURE I

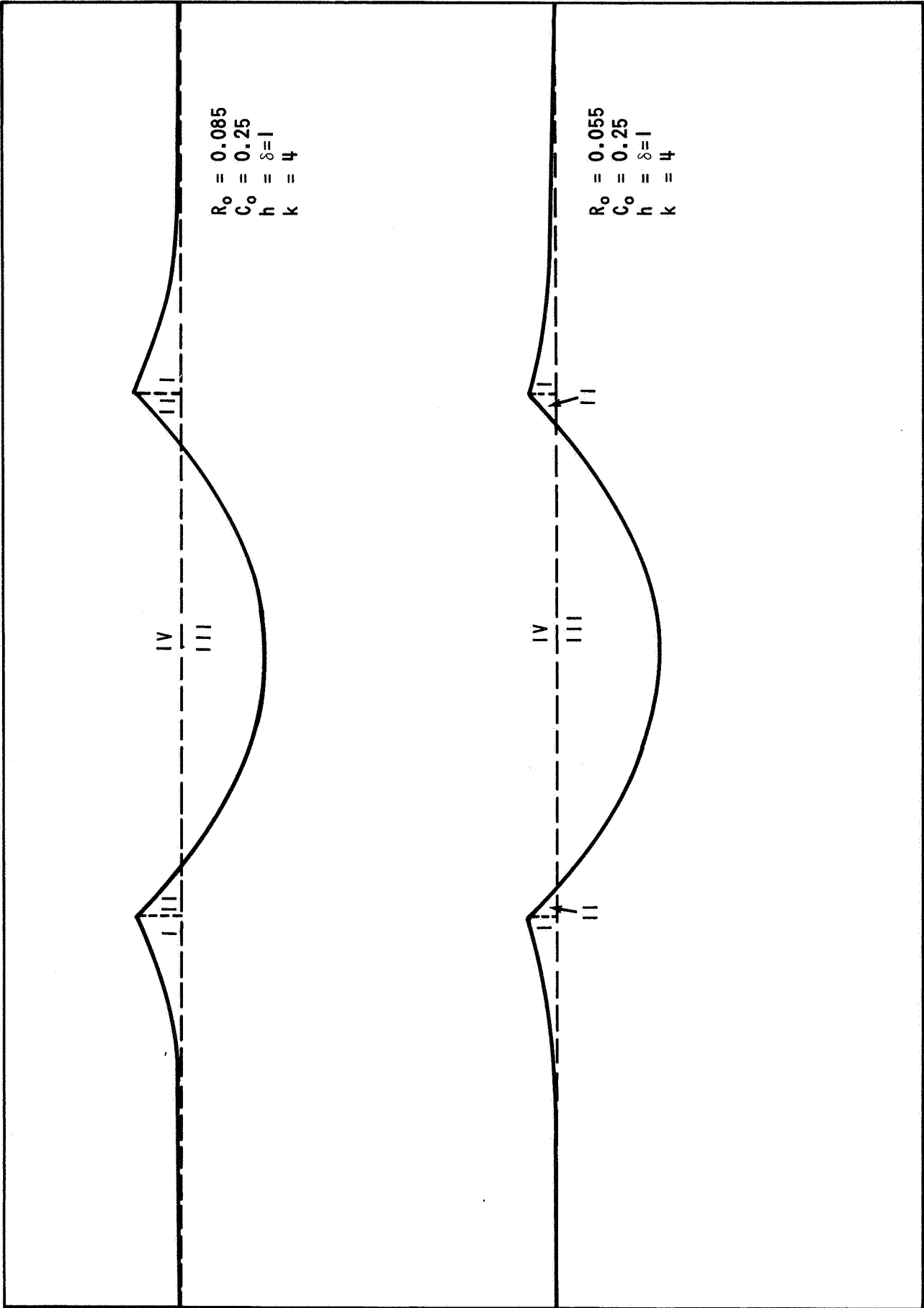


FIGURE 2

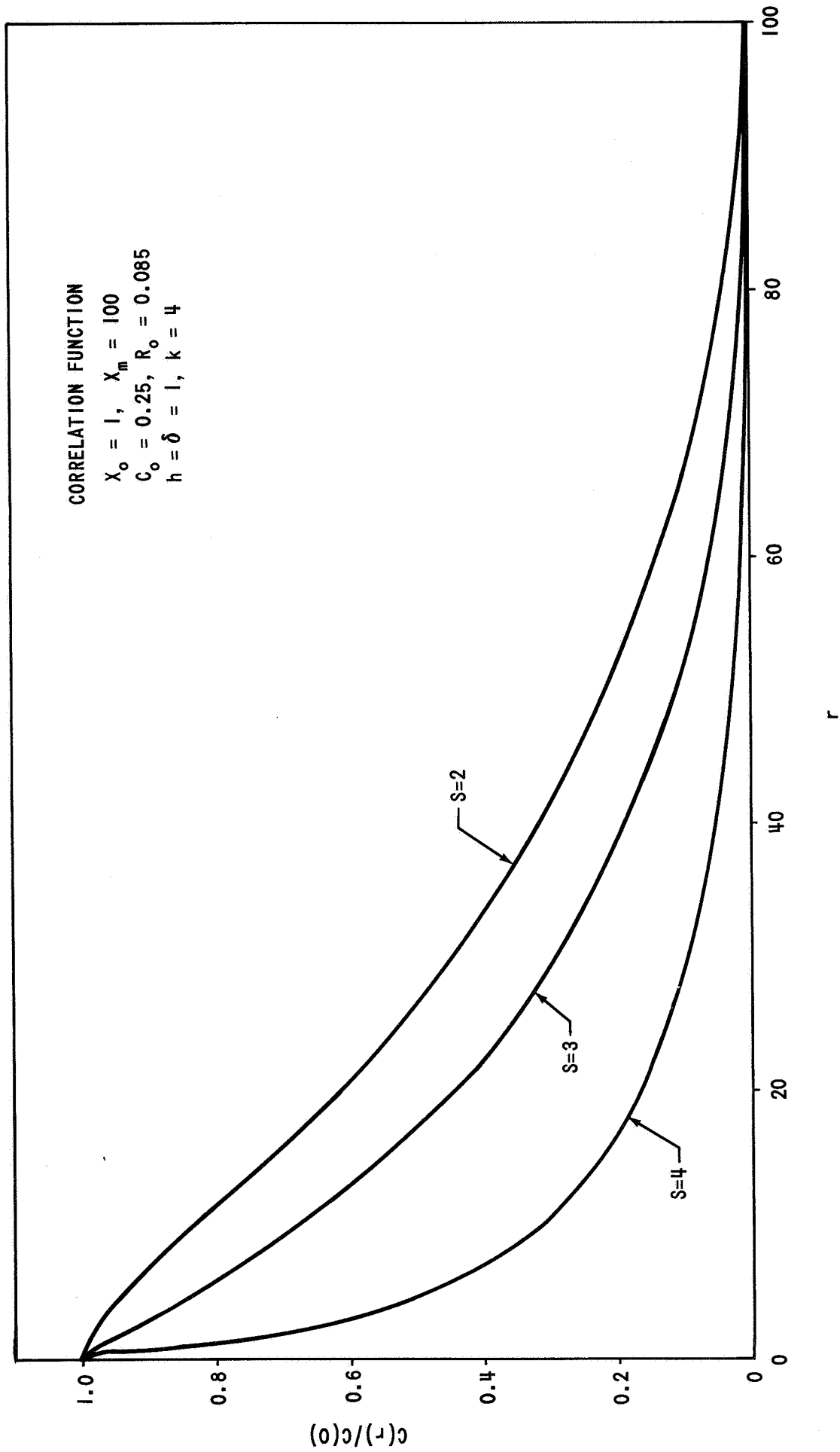


FIGURE 3

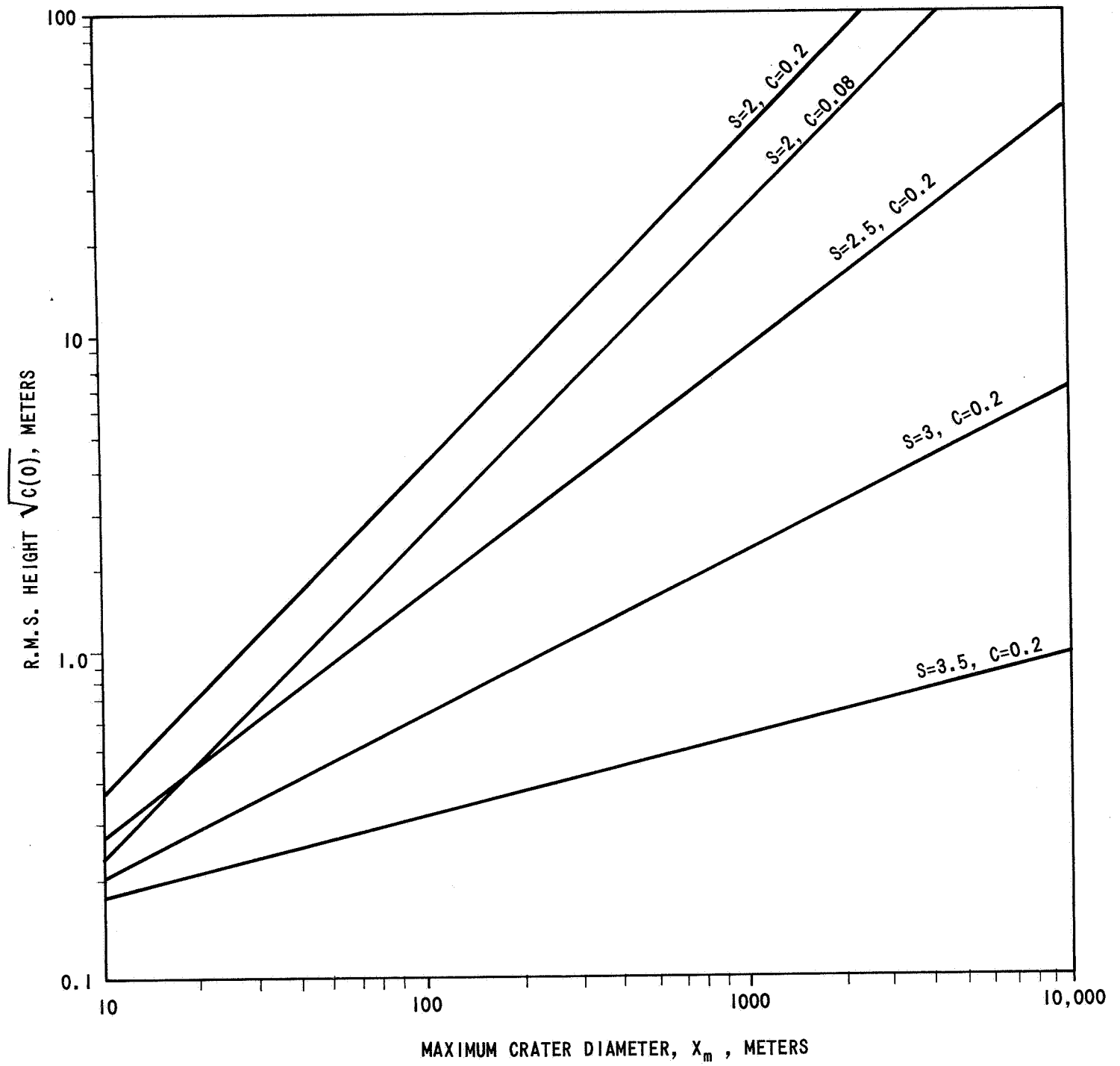


FIGURE 4

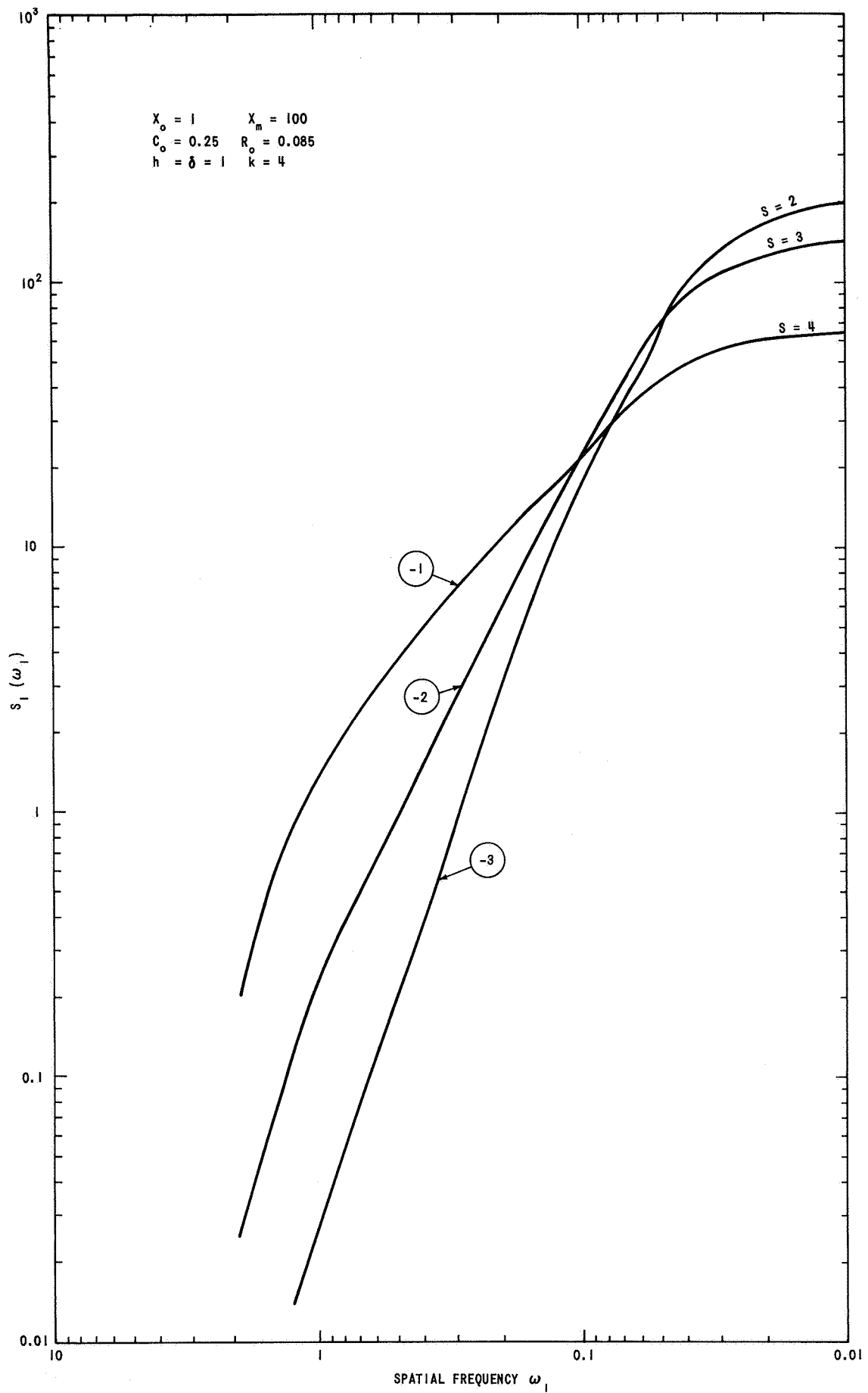


FIGURE 6 ONE DIMENSIONAL POWER SPECTRAL DENSITY (NORMALIZED)

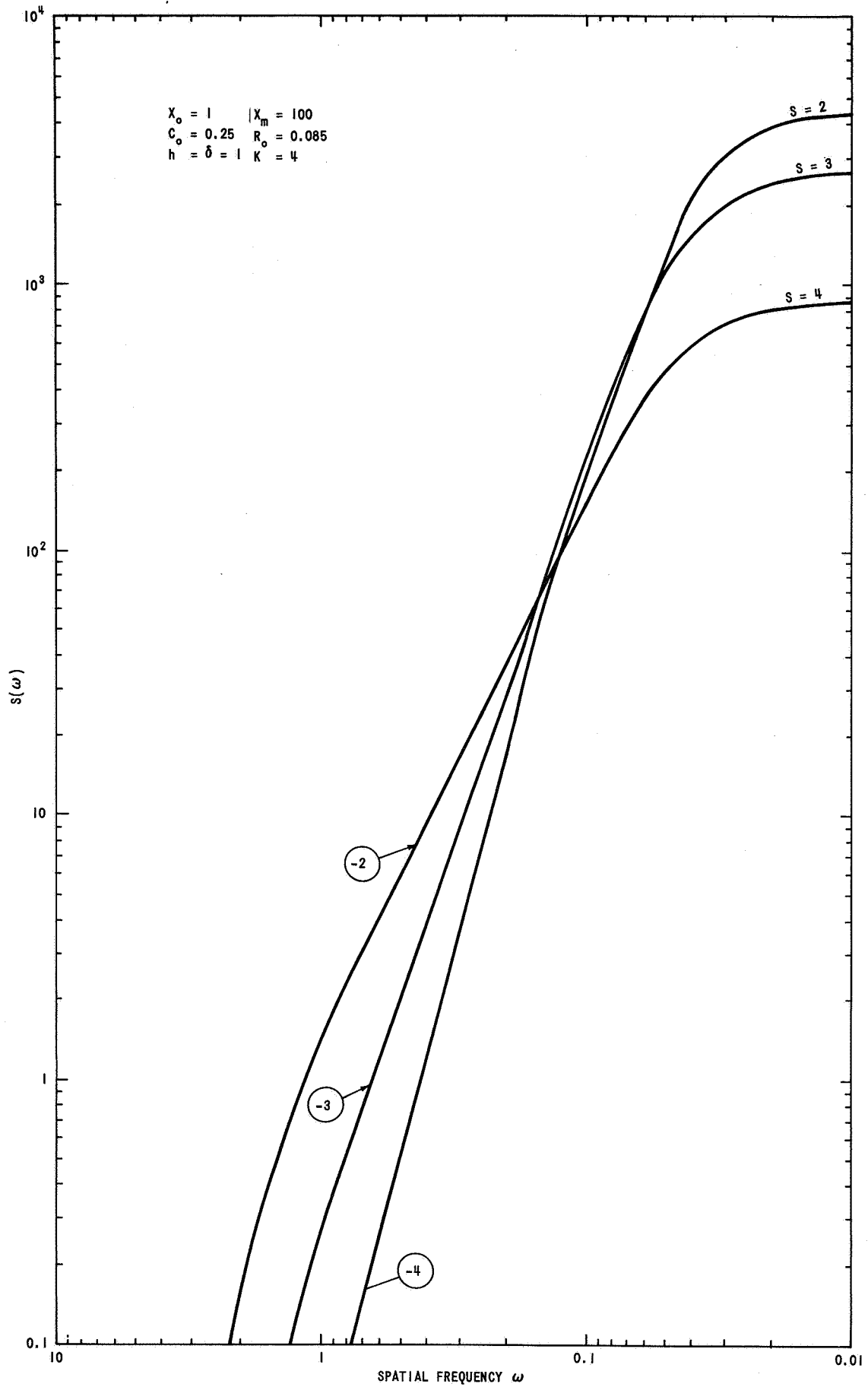


FIGURE 5 TWO-DIMENSIONAL POWER SPECTRAL DENSITY (NORMALIZED)

ACKNOWLEDGMENTS

I am very grateful to Mr. Robert Singers for programming the complicated numerical integrations needed in computing the functions $c(r)/c(0)$. I am also grateful to Miss Carol Banick for computing the functions $S(\omega)$ and $S_1(\omega_1)$.

DISTRIBUTION LIST

Complete Memorandum to

NASA Headquarters

Messrs. R. J. Allenby/MAL
 E. M. Davin/MAL
 L. E. Day/MAT
 D. P. Hearsh/SL
 J. K. Holcomb/MAO
 T. A. Keegan/MA-2
 D. R. Lord/MTD
 B. Milwitzky/MAL
 M. W. Molloy/MAL
 G. A. Reiff/SL
 L. Reiffel/MA-6
 L. R. Scherer/MAL
 J. B. Skaggs/MAP
 J. H. Turnock/MT
 G. C. White, Jr./MAR
 V. R. Wilmarth/MAL

NASA Hqs. Library - USS-10 (2)

Ames Research Center

Messrs. D. E. Gault/204-3
 V. R. Oberbeck/204-3
 W. L. Quaide/204-3
 L. Roberts/202-5

Goddard Space Flight Center

Dr. J. A. O'Keefe/640

Marshall Space Flight Center

Messrs. J. A. Downey/R-RP-J
 E. Stuhlinger/R-RP
 O. H. Vaughn, Jr./R-AERO-Y

Manned Spacecraft Center

Messrs. P. B. Burbank/TG
 J. E. Dornbach/TH3
 J. M. Eggleston/TH
 T. Giuli/TG5
 W. N. Hess/TA
 J. H. Sasser/TH3

Complete Memorandum to

U.S. Geological Survey

Messrs. H. J. Moore
 R. J. Pike
 L. C. Rowan
 E. M. Shoemaker
 N. Trask

Jet Propulsion Laboratory

Mr. J. D. Burke/180-302

Bendix Aerospace Systems Division

Mr. K. H. Wadleigh

Oliver Machinery Co.

Dr. R. B. Baldwin

University of Arizona

Messrs. G. Fielder
 W. K. Hartmann
 R. G. Strom

California Institute of Technology

Messrs. R. B. Leighton
 B. C. Murray
 T. McCord

Harvard University

Messrs. J. Pollack
 C. Sagan

Smithsonian Astrophysical Observatory

Mr. C. R. Chapman

DISTRIBUTION LIST

Complete Memorandum to
University of Manchester

Dr. Z. Kopal

University of Maryland

Dr. E. J. Opik

Melpar, Inc.

Dr. T. P. Meloy

Lincoln Laboratory

Drs. J. V. Evans
T. Hagfors

General Motors Defense
Research Labs.

Messrs. S. Romano
D. J. Schuring

University of Houston

Dr. H. S. Hayre

National Radio Astronomy
Observatory

Dr. D. Buhl

Environmental Science Services
Admin. (ESSA)

Dr. W. K. Klemperer

University of Colorado

Dr. P. Beckmann

Complete Memorandum to
Bellcomm, Inc.

Messrs. F. G. Allen
G. M. Anderson
G. R. Andersen
D. J. Belz
A. P. Boysen, Jr.
J. O. Cappellari, Jr.
D. A. Chisholm
T. H. Crowe
C. L. Davis
D. A. De Graaf
J. S. Dohnanyi
J. P. Downs
D. R. Hagner
P. L. Havenstein
W. G. Heffron
H. A. Helm
N. W. Hinners
B. T. Howard
D. B. James
J. Kranton
K. E. Martersteck
R. K. McFarland
J. Z. Menard
V. S. Mummert
L. D. Nelson
G. T. Orrok
R. V. Sperry
W. Strack
J. W. Timko
J. M. Tschirgi
R. L. Wagner
J. E. Waldo

All Members Department 2015
Department 1023
Central File
Library

Abstract Only to

Bellcomm, Inc.

Copy to
Mr. I. M. Ross